Dynamic Mechanical Properties of Austenitic Stainless Steels — Fitting of Experimental Data on Constitutive Equations

C. Albertini, M. Montagnani
Commission of the European Communities, J.R.C. Ispra Establishment, Applied Mechanics Division, I-21020 Ispra (Varese), Italy
R. Cenerini, S. Curioni
Università di Bologna, Facoltà di Ingegneria, Via Risorgimento 2, I-40100 Bologna, Italy

Summary

The design of reactor structures for containment of extreme dynamic loading conditions requires the knowledge of dynamic mechanical properties of materials damaged up to end-of-life conditions by welding, creep thermal and mechanical fatigue and irradiation, under multiaxial loading conditions. The experimental data given by engineering and physical tests are the basis for the formulation of constitutive laws which must be calibrated by applying best fitting techniques to the experimental data. Once the constitutive law is well founded on such data, its prediction capability will be checked by further experiments concerning loading and deformation histories representing those of the real structure: rapidly changing strain rates, repeated loading and unloading, reversed reloading and wave propagation and reflection. At this time, constitutive laws can be implemented in computer codes, and the design criteria, such as safety coefficients, maximum allowable stress, strain and strain rate, can be established.
These guidelines have been followed in our research by:

- developing the experimental techniques, based on a split tension bar and a hydropneumatic machine, allowing the performance of uniaxial tensile tests at strain rates up to 1000 per second, on small and near-real size specimens (cross sections of the specimen from 7 to 5000 mm^2);
- extending the same test equipment to biaxial stressing;
- performing a screening uniaxial tensile test programme on small specimens (7 mm^2 cross section) of austenitic stainless steels in virgin, welded, thermally aged, fatigued and irradiated (up to 2 dpa) conditions;
- by studying some models of constitutive laws which promise to represent the observed phenomena.

This line of research has been followed for the characterization of AISI 316 and other austenitic steels. The results obtained are presented and discussed.
While at room temperature all virgin and damaged materials show a dynamic hardening behaviour with dynamic flow curves above the static one, at high temperature (400 and 550°C), the dynamic flow curves of virgin austenitic steels passes from a substantial dynamic hardening to dynamic softening. At high temperature materials damaged by welding, thermal aging and irradiation always show dynamic softening. This spread of dynamic response of austenitic stainless steels leads to structures whose components have very different dynamic mechanical properties. This mis-match of dynamic mechanical properties, often not observed in static tests, leads to stress and/or strain concentrations in the real structure whose effects can be investigated only by testing near-real size specimens under multiaxial loading conditions. In the near-real size specimens, the effects of temperature rise of the material during dynamic deformation (adiabatic process) can also be investigated.
Taking as a basis the theory of Perzyna, a calibration procedure has been developed for the determination of all parameters necessary to define the constitutive relationship of AISI 316, using the experimental results previously described, which are determined by tests at constant strain rate, at both ambient and high temperature (400°C). Experimental results and the calibrated curve fit fairly well, considering the limited number of experimental data available.
As far as the Bodner equation is concerned, a calibration procedure has been described.

1. Introduction

The need to reduce structure costs both for nuclear reactors and for other constructions means that it is necessary to reduce the margin of uncertainty of the calculations for the structures themselves, while maintaining, or even in some cases increasing, safety margins. It is thus a prerequisite to identify the constitutive equations of the materials involved. The constitutive equation, which in its final expression is a mathematical formulation, can be introduced into modern calculation codes for mechanical structures through suitable adaptations of existing codes.

In the case of an accident, for the calculation of the structures which are designed to contain the effects of dynamic accident loads, one must know the constitutive equation of the materials, i.e. the link between stresses and deformation, as a function not only of the temperature but also of the deformation rate up to high values, which in the case of the thermal excursions of the core of a fast reactor reach strain rates up to $\dot{\epsilon} = 1000\ s^{-1}$ and in the case of hard missile impact strain rates up to $\dot{\epsilon} = 10^5\ s^{-1}$, Olson [1].

The constitutive equation is identified for a particular reference material so as to reduce in the research phase the effects of the various characteristic parameters of the material which influence its resistance, ductility, etc. Obviously the design of a nuclear reactor or of any other mechanical construction cannot be restricted to the use of a material thus selected because of cost and supply problems. It should be noted, Wood [2], that even for a highly selected component alloy such as an AISI austenitic steel, large scatters can be seen from one batch to another, depending on slight differences in composition, different manufacturing histories and so on.

Thus we reserve for the period after the determination of the constitutive equation of a well-determined sample material the study of the spread of experimental results which is obtained with materials of different origins. This is vital because this spread can reduce the safety margins with respect to the sample material and thus it is necessary to give the manufacturer a definite basis for the safety of the structure which has been designed.

The various phases followed by us to determine the constitutive equations of AISI 316 are as follows:
Among the various constitutive equations which the theoreticians have developed, Maier [3], to describe the behaviour of the materials, some were selected which it was felt would describe the materials in a fairly wide range of deformation rates which go from sector II to sector IV of the diagram described by Rosenfield and Hahn [4]. Of these formulations we have oriented the research towards those which were of greatest interest for the physical foundation of the basic formulation of the constitutive law, for example the formulations of Bodner [5] and Perzyna [6].

Perzyna's formulation is like a reference framework founded on both engineering and fine structure considerations. This general framework is thus "compatible" with the experimental results obtained for a rather wide range of similar materials and is thus able to describe the experimental stress strain diagrams obtained at various temperatures and strain rates and with the physical laws which govern this behaviour (deformation mechanisms based on a process of thermal activation and also on dissipative mechanisms).

The constitutive equations thus selected contain various parameters which allow them to be applied over a vast range of materials and experimental conditions. These parameters are calibrated with the specific experimental results from the materials in which we are interested. Thus it is verified that the equations are compatible with the materials selected by us for the investigation: these have been tested in the ranges of σ, ϵ, $\dot{\epsilon}$, T which are of particular interest to reactor constructors.

Once the constitutive equation has been calibrated it can, to a first approximation, be implemented in computer programs. However, given the multiplicity of the material variables, it is as well to verify the constitutive equations gradually through further tests and examinations. These are:

- special $\dot{\epsilon}$ histories;
- particular states of stress and strain (e.g. monoaxial, bi- and triaxial);
- temperature histories;
- presence of defects, either natural or arising during operation (welds, ageing, creep, fatigue, irradiation, etc.);
- influence of particular chemical constituents, batches, etc.;
- other possible operating conditions, size of the structure, adiabatic heating, etc.

From these particular phenomena one must determine an appropriate evolution function again based on the observation of the microscopic behaviour and on experimental tests, and it must be verified if these new functions are compatible with the base model.

A close collaboration between theoreticians and experimentalists is therefore necessary. This must lead to a final result which will be of practical use to the constructor.

2. Experimental procedures and results obtained

The experimental techniques used were taken from a vast preceding literature in which various authors, Hopkinson, Davies, Kolsky, Wood, Malvern, Campbell, Lindholm, et al. [7,8,9,10,11,12] have developed apparatus to test materials at high deformation rates. Inspired by these authors we have developed the devices which we have used for characterization of the materials for nuclear reactors, Albertini, Montagnani [13].

The devices developed for the monoaxial tension tests were as follows:

- a hydropneumatic machine for strain rates between 10^{-1} and 10^{2} s^{-1};
- a modified Hopkinson bar for strain rates up to 10^{3} s^{-1}.

Conventional equipment was used for low strain rates.

For a preliminary calibration of the Perzyna and Bodner formulations we have submitted an AISI 316H (JRC reference material, see Table 1) and an AISI 316L to dynamic tensile tests at constant strain rate, strain rates ranging from 10^{-3} to 10^{3} s^{-1}, and test temperatures 20, 400 and 550°C. The results of this test programme, as far as AISI 316H is concerned, are shown in Figs. 1 to 6:

- at 20°C the flow curves show an enhanced dynamic hardening and reduction of ductility (i.e. uniform strain, fracture strain) with increasing strain rate (Figs. 1 and 2);
- at 400°C with increasing strain rate the flow curves show dynamic hardening during uniform deformation, small oscillations of ultimate tensile strength around the static value, and a small reduction of uniform strain and fracture strain (Figs. 3 and 4);
- at 550°C with increasing strain rate the flow curves show a slight dynamic hardening during uniform deformation, no changes of ultimate tensile strength, a small reduction of uniform strain, and a small increase of fracture strain (Figs. 5 and 6).

At room temperature the dynamic hardening behaviour has been observed for all the austenitic stainless steels tested up to now in our laboratory (AISI 316L, AISI 321, AISI 304, AISI 347, AISI 316 20% CW) as reported at SMIRT VI, Albertini, Montagnani [14], for both virgin and damaged conditions.

In the same paper it was stated that the virgin austenitic stainless steels tested at the working temperatures (400 - 550°C) showed large variations in the mechanical properties on passing from one material to another. In fact, from a dynamic hardening behaviour (AISI 316H at 400 and 550°C and AISI 316L at 400°C) one passes to practically no strain rate sensitivity (AISI 304L at 400 and 550°C and AISI 316L at 550°C), to slight dynamic softening (DIN 4981 at 490°C).

Furthermore the same austenitic stainless steels damaged by welding, thermal ageing and irradiation, tested at 400 and 550°C, showed a dynamic softening behaviour and reduction of ductility which indicate that the micro-defects induced by the different damaging processes govern the dynamic response of these damaged materials in the same way.

Our results were compared with those obtained mainly by Steichen [15] and Isozaki [16] on similar steels by dynamic tensile tests. The results of this comparison were in good agreement.

The case of monotonic loading is the most probable case of loading during an accident due to core expansion. If waves are transmitted they may create conditions of loading, unloading and reverse loading which can be complicated by hysteresis effects (e.g. Bauschinger effect). These are the main topics to be studied in our test programme. With a view to the fact that the hypothetical accident produces a multiaxial state of stress in the structures, enhancing the differences in dynamic mechanical properties between virgin and damaged materials due to anisotropy, some dynamic biaxial testing apparatus have been also developed, Albertini, Montagnani [17]. These devices, acting on small cruciform specimens having a cross section up to 20 mm^2, at strain rates up to 10^{3} s^{-1}, also make it possible to give an experimental answer to the problem of yield and fracture criteria. In fact, the yield criteria, up to now, have proved to be efficient under static conditions, for very small deformations, and for isotropic materials. For the moment these experiments are under development and experimental data are not available.

We are also developing highly sensitive interferometric methods, capable of measuring strain distribution as a function of time, directly on the specimen, in order to distinguish the effects of dynamic softening and restriction of area instabilities.

The physical characterization of the microstructure and defect parameters which determine the observed mechanical phenomena requires the support of electron microscopy, X-ray diffraction and neutron scattering measurements, in order to be able to observe which microstructural defects are responsible for each engineering phenomenon, Albertini, Montagnani [18].

In order to perform investigations on the effect of size on the mechanism of deformation, our laboratory., on the basis of the experience gained by testing small specimens, has developed a dynamic biaxial apparatus with a maximum load of 5 MN and 40 ms pulse duration, capable of performing tests on large specimens with cross

sections up to 5000 mm². The apparatus has been constructed at JRC-Ispra in a version adapted to preliminary monoaxial testing and is now operational for a preliminary test programme [18].

3. Calibration of the constitutive laws

The essential characteristics of the constitutive laws of Bodner and Perzyna have been studied and summarised by Albertini et al. [19]. Their fields of application and the fundamentals of the main functions making up their constitutive equations have been described. It should be remembered that Perzyna [6] has recently presented a modified theory of viscoplasticity in which the elastic-viscoplastic formulation seems to be the most promising for time dependent modelling of structural materials when strain rates of 10^3 s^{-1} may be found in accident conditions. In these problems the material behaviour is governed by plastic as well as by rheological effects. Usually the term elastic-viscoplastic is reserved for materials showing viscous properties in the plastic region only. This idealization to which we refer presently simplifies the argument considerably and can be accepted when rheological effects are more pronounced after the plastic state is reached. The determination of the yield condition for a material showing viscous properties in the elastic and plastic regions is very difficult, while it is much easier when viscous properties are found only in the plastic region. Let us consider an incompressible perfectly plastic material; in classical plasticity, plastic flow takes place when a yield condition is satisfied and the following relations hold:

$$\dot{\epsilon}^{p}_{ij} = \lambda S_{ij} \tag{1}$$

$$\lambda = \frac{I_2}{J_2} \tag{2}$$

where:

$\dot{\epsilon}^{p}_{ij}$ is the plastic strain rate tensor

S_{ij} is the deviatoric stress tensor

I_2^2 is the second invariant of the plastic strain rate tensor

J_2^2 is the second invariant of the deviatoric stress tensor.

With the Von Mises yield condition:

$$J_2 = \frac{\sigma_y}{\sqrt{3}} \tag{3}$$

where σ_y is the uniaxial yield stress, eq.(1) becomes:

$$\dot{\epsilon}^{p}_{ij} = \frac{I_2 \sqrt{3}}{\sigma_y} S_{ij} \tag{4}$$

Equation (4) and (3) are the basis of elastic plastic analysis. If $J_2 < \sigma_y / \sqrt{3}$, then λ and $\dot{\epsilon}^{p}_{ij}$ are zero.

A viscoplastic constitutive law could be obtained from (4) by stipulating that a relationship exists between I_2 and J_2. Forms for this relation may be obtained by the dynamics of dislocations, which shows that dislocation velocity, and therefore plastic strain rate, is a function of stress.

The strain rate sensitivity behaviour of metals can be divided into two regions [4]:

. the thermally activated region;

. the phonon damping region.

For example, in mild steel for strain rates up to 10^3 s^{-1}, thermoactivation phenomena prevail. For isotropic work hardening materials Perzyna [6] proposed the following equation, for a given temperature:

$$\dot{\epsilon}^{p}_{ij} = \frac{\gamma}{\varphi\left(\frac{I_2}{I_2^s} - 1\right)} < \Phi\left(\frac{J_2}{K} - 1\right) > \frac{S_{ij}}{J_2} \tag{5}$$

where:

I_2^S	is called the static value of strain rate measure and is the value such that for a test under combined stress conditions with $I_2 \leqslant I_2^S$ no rate sensitivity effect is observed;
K and γ	are material parameters, functions of ϵ^p;
Φ	is a material function;
φ	is a control function;
K, γ, Φ, φ	have to be determined by a best fit to the experimental data.

Symbol:

$$< \Phi \left(\frac{J_2}{K} - 1\right) > = \begin{cases} 0 \text{ if } \left(\frac{J_2}{K} - 1\right) \leqslant 0 \\ \Phi \text{ if } \left(\frac{J_2}{K} - 1\right) > 0 \end{cases}$$

Equation (5) may also be written in the form

$$J_2 = K \left\{1 + \Phi^{-1} \left[\frac{I_2}{\gamma} \varphi \left(\frac{I_2}{I_2^S} - 1\right)\right]\right\} \tag{6}$$

Often functions Φ^{-1} and φ are well approximated by power functions. An application of (6) was made [6] to tension-torsion experimental data of Lindholm [12] on mild steel, which is well approximated by:

$$J_2 = K \left\{1 + \left[\frac{I_2}{\gamma} \left(\frac{I_2}{10^{-6}} - 1\right)^{1/5}\right]^{1/5}\right\} \tag{7}$$

where:
K = 21.50 Ksi
γ = 25.82 s^{-1}.

Equation (6) of course holds in uniaxial geometry in the form:

$$\sigma = K \left\{1 + \Phi^{-1} \left[\frac{\dot{\epsilon}^p}{\gamma} \varphi \left(\frac{\dot{\epsilon}^p}{\dot{\epsilon}^s} - 1\right)\right]\right\} \tag{6bis}$$

For a one-dimensional state of elastic-viscoperfectly plastic material and ignoring the φ function, eqs.(5) and (6) become respectively:

$$\dot{\epsilon}^p = \gamma < \Phi \left(\frac{\sigma}{\sigma_y} - 1\right) > \tag{8}$$

$$\sigma = \sigma_y \left[1 + \Phi^{-1} \left(\frac{\dot{\epsilon}^p}{\gamma}\right)\right] \tag{9}$$

When the material is work hardening, eqs.(8) and (9) become:

$$\dot{\epsilon}^p = \gamma < \Phi \left[\frac{\sigma}{\sigma_s(\epsilon^p)} - 1\right] > \tag{10}$$

$$\sigma = \sigma_s(\epsilon^p) \left[1 + \Phi^{-1} \left(\frac{\dot{\epsilon}^p}{\gamma}\right)\right] \tag{11}$$

where $\sigma_s(\epsilon^p)$ represents the static stress-strain relation in the one-dimensional case. Equation (10) was first introduced by Malvern [10], under special conditions.

It is worthwhile to consider that the γ and K parameters of eqs.(5) and (6), denoting viscosity coefficient and a strain dependent parameter, respectively, may also depend on temperature and on imperfections (notches, welding, radiation, creep, fatigue). The possibility of introducing defects in constitutive equations is very interesting for long term high-temperature aging materials since this allows one to consider actual operating conditions and safety coefficients in the end-of-life condition when significant material damage can be expected.

As far as calibration of eq.(6) of Perzyna is concerned, the experimental data $\sigma = \sigma(\epsilon)$ for different strain rates are to be transformed into the more suitable form: $\sigma = \sigma(\epsilon^p)$ for ϵ = const. Moreover, the values of true stress and true strain $\sigma_t = \sigma_t(\epsilon_t)$ should be considered instead of the rough experimental values $\sigma = \sigma(\epsilon)$ related to engineering stress and strains. Conversion formulas used from engineering to true values are:

$$\epsilon_t = \ln (1 + \epsilon) \qquad (12)$$

$$\sigma_t = (1 + \epsilon)\,\sigma$$

From the diagrams of Figs. 1 to 6 regarding AISI 316H, it can be seen that up to values of ϵ of 20% there is no necking effect, and thus the two preceding expressions can be considered to be valid. This has been verified by observation with a fast camera.

The static value $\dot{\epsilon}_s$ of strain rate (i.e. the strain rate value such that for $\dot{\epsilon}^p \leqslant \dot{\epsilon}_s$ no rate sensitivity effect is observed, see eq.(6bis)) was assumed:

$$\dot{\epsilon}_s = 10^{-3}\ s^{-1}.$$

A least square technique was used in order to find out the material constants from experimental data. A Levenberg-Marquardt routine was applied. The problem is stated as follows: given M non linear functions f_1, f_2, f_M of a vector parameter $\underset{\sim}{X}$, minimize over $\underset{\sim}{X}$:

$$f_1(\underset{\sim}{X})^2 + f_2(\underset{\sim}{X})^2 + \ldots, f_M(\underset{\sim}{X})^2$$

where:
$\underset{\sim}{X} = (X_1, X_2, \ldots, X_N)$ is a vector of N parameters to be estimated. Let $\underset{\sim}{X}^0$ be an initial estimate of $\underset{\sim}{X}$. A sequence of approximations to the minimum point is generated by:

$$\underset{\sim}{X}^{n+1} = \underset{\sim}{X}^n - [\alpha_n D_n + J_n^T J_n]^{-1}\ J_n^T \underset{\sim}{f}(\underset{\sim}{X}^n)$$

where:

J_n is the numerical Jacobian matrix evaluated at X^n
D_n is a diagonal matrix equal to the diagonal of $J_n^T J_n$
α_n is a positive constant (Marquardt parameter).

Equation (6bis), assuming as a first approximation for Φ^1 and φ functions exponential form based on the trend of the experimental curves, becomes:

$$\sigma = K\,\{1 + [\frac{\dot{\epsilon}^p}{\gamma}(\frac{\dot{\epsilon}^p}{10^{-3}} - 1)^{1/n}]^{1/n}\} \qquad (13)$$

The least square technique gives the curves shown in Figs. 7, 8, 9 and 10 regarding AISI 316H and AISI 316L tested at 20 and 400°C, obtained by fixing initially the value of the coefficient n on the basis of preceding experiments with similar materials. One then calculates the parameters γ and K for some values of ϵ (see Table 2) and thus one rechecks whether the coefficient n chosen preliminarily produces a constitutive curve fitting the experimental data. On the basis of this comparison the selected n is confirmed or not, and found to be incorrect one can tentatively assume another one, repeating the cycle until a satisfactory result is obtained.

Finally then all three parameters, n, γ and K are optimized on the basis of the experimental results. The dependence of K and γ on the strain is described for K by a linear law and for γ by an exponential law as shown in Figs. 11 and 12, and in Table 3 reporting also the confidence levels reached. The $\sigma = \sigma(\dot{\epsilon}^p)$ curves for ϵ = const. are thus calculated using the appropriate values n, K and γ (see Figs. 13 to 16) and are comparable with those determined from the best fitting of the experimental data with an average scatter $\leqslant \pm 3.5\%$ (Table 4).

The links between σ, ϵ, $\dot{\epsilon}$ for the materials used and for a prechosen temperature, are uniquely determined on the basis of such relationships. A successive stage in the research could be that of establishing the law of dependence of K and γ on the temperature T, as well as on ϵ, thus producing constitutive diagrams which are functions of σ, ϵ, $\dot{\epsilon}$ and T. One could thus introduce the dependence of K and γ from the concentration of defects for defective materials.

We should remember that Perzyna and Pecherski have recently produced a calibration [20] of their constitutive laws based on the experimental data already published by us [18] for AISI 316L, following a procedure similar to ours, obtaining results which are in good agreement with those reported here by us.

Using the calibrated Perzyna formulation, given a strain rate history $\dot{\epsilon}(t)$, the corresponding σ,ϵ diagram can be calculated and implemented in the actual calculation codes.

The formulation proposed by Bodner [5] is based on assuming that elastic and inelastic deformations take place at every stage of loading and unloading. An appropriate decomposition of the stress and deformation rate tensors

makes it possible to formulate an elastic-viscoplastic theory that does not require a predetermined yield condition. For an elastic-perfectly viscoplastic material, Bodner suggested that a relationship between I_2 and J_2 of the form

$$I_2^2 = I_0^2 \exp\left[-\frac{Z^2}{3}/J_2^2\right]^n \quad \text{should be inserted in eq. (4),} \tag{14}$$

where I_0, Z and n are material constants to be determined by experiments. I_0^2 is the maximum value of the second invariant of the plastic strain rate; smaller values of the viscoplastic coefficient I_0 correspond to a lower proportion of stored elastic energy. Z is a "hardness" coefficient giving the material resistance to deformation, and corresponds in a general way to the yield stress, but lacks a direct correspondence with the usual definition of yield stress. n is connected with the strain rate sensitivity.

When work hardening is to be considered, the resistance must increase with plastic flow, which means that I_2 should vary inversely with the measure of strain hardening. Bodner suggested that the most significant state variable to represent this property is the plastic work W_p, and a dependence of parameter Z on W_p was introduced.

For uniaxial straining of a simple rod, the constitutive equation for a work hardening material proposed by Bodner is:

$$\dot{\epsilon}_p = \frac{2\,I_0}{\sqrt{3}} \frac{\sigma}{|\sigma|} \exp\left\{-\frac{1}{2\sigma^{2n}}\left[\bar{Z} - \Delta Z \exp\left(-m\int\sigma\dot{\epsilon}_p dt\right)\right]^{2n}\right\} \tag{15}$$

Plastic work $W_p = \int\sigma\dot{\epsilon}_p dt$ is introduced in the expression of Z through the formula:

$$Z = \bar{Z} - \Delta Z \exp\left(-m\,W_p\right) \tag{16}$$

The parameter

$$Z_0 = \bar{Z} - \Delta Z$$

gives the "originary resistance", i.e. is the value of Z when plastic work is zero. The parameter m is related to strain hardening; for higher values of m, the value of Z corresponding to a certain plastic work figure is also greater. The five constants (I_0, $\bar{Z}$, Z_0, m and n) appearing in (15) can be determined for a particular material by a best fit of test results at two constant rates of extension. Bodner calibrated his constitutive equation for titanium. Constitutive eq.(15) may also be written in multiaxial geometry:

$$\dot{\epsilon}_{ij}^{p} = \frac{S_{ij}}{J_2} I_0 \left\{\exp\left[-\left(\frac{1}{3J_2}\right)^n \left(\bar{Z} - \Delta Z \exp\left(-m\,W_p\right)\right)^{2n}\right]\right\} \tag{17}$$

where material constants are the same as in eq.(15).

Research is still necessary to find the most appropriate analytical and numerical tools for calibration of the constitutive equation of Bodner. A possible procedure was suggested by Maier [3]. It requires measuring at least two $\sigma(\epsilon)$ curves for two different strain rates, and considering at least three (σ_i, ϵ_i^p) couples for each curve.

Working out eq.(15) by assuming $\dot{\epsilon}^p$ = const., an equation in the implicit form $f(\sigma,\epsilon,\dot{\epsilon}^p$, material constants) =0 may be obtained in algebraic terms (and not in evolution form like eq.(15). Assuming arbitrarily the I_0 parameter, a set of transcendental equations are obtained which allow the material constants (m, n, Z, Z_0) to be determined from the 6 couples (σ_i, ϵ_i^p). A higher precision may be obtained when more (σ_i, ϵ_i^p) values are considered and more than two $\sigma(\epsilon)$ curves are measured. The equation set has then to be solved by a least squares technique in order to obtain the material constants.

One should observe that, in principle, uniaxial experimental data (when they cover the proper parameter ranges) are sufficient for calibration of constitutive equations, even for multiaxial geometry. In fact, the material constants and functions are the same in the uniaxial and multiaxial formulations of constitutive equations as may be seen by comparing eq.(6) with (6bis) and eq.(15) with (17). Nevertheless, biaxial measurements are very important as they allow a check of multiaxial constitutive equations formulations and of material constants.

4. Conclusions and outlines of future work

In this paper we have shown how, based on the preceding work of various researchers, we have constructed a series of specific apparatus for the tests on materials, virgin and defective, which are used in nuclear reactors for a σ, ϵ and $\dot{\epsilon}$ range and a stress pattern compatible with the usage requirements of the said materials.

We have presented the results found for AISI 316L and 316H and other austenitic materials. The results

obtained by us and the results from the literature show that the behaviour of such steels under monotonic dynamic loading moves from an accentuated dynamic hardening to dynamic softening, particularly in the case of damaged steels. Using Perzyna's formulation it was possible to represent the relationship σ, ϵ, $\dot{\epsilon}$ at temperatures of 20 and 400°C, for AISI 316L and 316H steels which show the phenomenon of dynamic hardening, with a satisfactory confidence level. For other materials which show dynamic softening (and for AISI 316L and damaged 316H which also show such phenomena) a particular adaptation of the constitutive equation based on the experimental results and on the theory of the development of defects must be developed.

Thus an adaptation may be found to be necessary taking account of the particular phenomena already mentioned in the introduction and taking account of the results of the multiaxial tests.

Close collaboration between the experimentalists and the theoreticians involved in constitutive formulations for an adaptation of the mathematical formulations of the real behaviour of the material, is necessary.

Perzyna's formulations considered here are not a rigid formulation but, in fact, allow developments to introduce new phenomena and observations of the basic mechanisms within the already existing general framework. As far as Bodner's formulation is concerned, one can observe that the method indicated for the calibration seems practical and it seems possible to use this constitutive formulation to obtain a comparison.

Acknowledgements

We are indebted to Prof. P. Perzyna for the orientation of our research, performed during several seminars held in Ispra, JRC and at the University of Bologna.

References

[1] G.B. Olson, "Adiabatic deformation and strain localisation", Shock Waves and High Strain Rate Phenomena in Metals, M. Meyers and L.E. Murr, 221-247, Plenum Press, 1981.
[2] D.S. Wood, "The tensile properties of austenitic steel weld metals", CEC Study Contract RAP-025-81-UK, not published.
[3] G. Maier, "Rate sensitivity, con particolare riguardo ai metalli", CEC Study Contract 915/78/07 SISPI, 1979, not published.
[4] A.R. Rosenfield, G.T. Hahn, "Numerical description of the ambient low-temperature, and high strain rate flow and fracture behaviour of plain carbon steel", Trans. ASM 59, 962-980, 1966.
[5] S.R. Bodner, Y. Partom, "Constitutive equations for elastic-viscoplastic strain hardening materials", J. Applied Mechanics, 42, 2, 385-389 (1975).
[6] P. Perzyna, "Modified theory of viscoplasticity. Application to advanced flow and instability phenomena", Arch. Mech., 32, 3, 403-420, Warszawa, 1980.
[7] R.M. Davies, "A critical study of the Hopkinson pressure bar", Phil. Trans. Roy. Soc. London Ser. A, 240, 375 (1948).
[8] H. Kolsky, "Stress waves in solids", Clarendon Press, Oxford, 1953 and Dover Publications 1963.
[9] D.S. Wood, D.S. Clark, Trans. Am. Soc. Metals, 43, 1951, 571
[10] L.E. Malvern, J. Appl. Mech., 18, 1951, 203.
[11] J.D. Campbell, "Dynamic plasticity: Macroscopic and microscopic aspects", Materials Science and Engineering, 12, 1973, 3-21.
[12] U.S. Lindholm, "Techniques of metals research", Vol. 5, Part 1, J. Wiley & S., 1971.
[13] C. Albertini, M. Montagnani, "Testing techniques based on the split Hopkinson bar," Inst. of Physics, Conf. Ser. No. 21, London, 1974.
[14] C. Albertini, M. Montagnani, "Experimental determination of material's constitutive laws and of design criteria of reactor structures in extreme dynamic loading conditions", Proc. SMIRT 6, Paper L 4/4, Paris, 1981.
[15] J.M. Steichen, "High strain rate tensile properties of AISI 304 stainless steel", J. of Eng. Mat. Techn. 1973, 7.
[16] T. Isozaki, T. Oba, "High velocity tensile test of austenitic stainless steel at elevated temperatures", Nucl. Eng. Des., 55, 1979, 375-387.
[17] C. Albertini, M. Montagnani, "Testing techniques in dynamic biaxial loading", Inst. Phys. Conf. Ser. No. 47, 25-34, 1979.
[18] C. Albertini, M. Montagnani, "Constitutive laws of materials in dynamics - Outline of programme of testing on small and large specimens for containment of extreme dynamic loading conditions", NED 68, 1981, 115-128.
[19] C. Albertini, R. Cenerini, S. Curioni, M. Montagnani, "Constitutive equations of austenitic stainless steels in dynamics. Experiments and calibration procedure", 1982, not published.
[20] P. Perzyna, R.B. Pecherski, "Modified theory of viscoplasticity. Physical foundations and identification of material functions for advanced strains", to be published.

TABLE 1

MATERIAL	Fabrication Process	CHEMICAL COMPOSITION											
		Cr	Ni	Mn	Mo	Nb	C	Si	S	P	Co	B	N
AISI 316 L	Solution treated plate 7 mm thick	16.0	13.3	1.82	2.74	<0.01	0.03	0.4	0.007	≤0.05	-	-	-
AISI 316 H	Mill-Annealed plate 50 mm thick	16.9	12.4	1.65	2.45	-	0.05	0.35	0.008	0.020	0.023	0.001	0.082

AISI 316 H 20° C, n = 7

$$\sigma = k(\varepsilon_t^p)\left[1+\left[\frac{\dot{\varepsilon}^p}{\gamma(\varepsilon_t^p)}\left(\frac{\dot{\varepsilon}^p}{10^{-5}}-1\right)^{1/n}\right]^{1/n}\right]$$

$K(\varepsilon_t^p) = 290 \cdot 2267 \bullet \varepsilon_t^p$ (MPa) Correlation Coeff. $r^2 = 0{,}99$

$\gamma(\varepsilon_t^p) = 3{,}676 \bullet 10^5 \exp(33{,}47 \bullet \varepsilon_t^p)$ (s^{-1}) $r^2 = 0{,}99$

AISI 316 H 400 ° C, n = 5,5

$K(\varepsilon_t^p) = 155 \cdot 1916 \bullet \varepsilon_t^p$ (MPa) Correlation Coeff. $r^2 = 0{,}99$

$\gamma(\varepsilon_t^p) = 1{,}198 \bullet 10^3 \bullet \exp(52{,}84 \bullet \varepsilon_t^p)$ (s^{-1}) $r^2 = 0{,}96$

AISI 316 L 20 ° C, n = 5

$K(\varepsilon_t^p) = 335 \cdot 1902 \bullet \varepsilon_t^p$ (MPa) Correlation Coeff. $r^2 = 0{,}99$

$\gamma(\varepsilon_t^p) = 6{,}175 \bullet 10^4 \bullet \exp(17{,}42 \bullet \varepsilon_t^p)$ (s^{-1}) $r^2 = 0{,}96$

AISI 316 L 400 ° C, n = 5

$K(\varepsilon_t^p) = 232 \cdot 2138 \bullet \varepsilon_t^p$ (MPa) Correlation Coeff. $r^2 = 0{,}97$

$\gamma(\varepsilon_t^p) = 3{,}174 \bullet 10^3 \bullet \exp(47{,}88 \bullet \varepsilon_t^p)$ (s^{-1}) $r^2 = 0{,}93$

TABLE 3

MATERIAL	$\varepsilon_1 = 0.2\%$		$\varepsilon_2 = 3.7\%$		$\varepsilon_3 = 5.5\%$		$\varepsilon_4 = 7.2\%$		$\varepsilon_5 = 9\%$		$\varepsilon_6 = 10.7\%$		$\varepsilon_7 = 14\%$		$\varepsilon_8 = 20.3\%$	
	$\dot{\varepsilon}(s^{-1})$	σ(MPa)	$\dot{\varepsilon}(s^{-1})$	σ(MPa)	$\dot{\varepsilon}(s^{-1})$	σ(MPa)	$\dot{\varepsilon}(s^{-1})$	σ(MPa)	$\dot{\varepsilon}(s^{-1})$	σ(MPa)	$\dot{\varepsilon}(s^{-1})$	σ(MPa)	$\dot{\varepsilon}(s^{-1})$	σ(MPa)	$\dot{\varepsilon}(s^{-1})$	σ(MPa)
AISI 316 H	0.004	267	0.004	388	0.004	422	0.004	455	0.004	484	0.004	512				
	0.082	306	0.082	430	0.082	466	0.082	502	0.082	529	0.082	557				
T = 20° C	0.88	357	0.88	470	0.88	504	0.88	535	0.88	563	0.88	595				
	4.5	371	4.5	494	4.5	527	4.5	565	4.5	593	4.5	624				
	45	368	45	493	45	530	45	567	45	605	45	631				
	480	430	480	547	480	585	480	611	480	638	480	672				
	750	471	750	574	750	605	750	635	750	659	750	683				
AISI 316 H	0.004	153	0.004	243	0.004	275	0.004	304	0.004	329	0.004	354				
	3.5	191	3.5	267	3.5	299	3.5	334	3.5	357	3.5	378				
T = 400° C	50	185	50	284	50	316	50	345	50	375	50	402				
	600	240	600	326	600	353	600	379	600	407	600	434				
	1000	253	1000	345	1000	374	1000	396	1000	411	1000	441				
AISI 316 L	0.004	278	0.004	420	0.004	490	0.004	550					0.004	613	0.004	713
	15	428	15	539.5	15	603	15	645					15	705	15	786
T = 20° C	44	435	44	599	44	664	44	702					44	769	44	850
	420	461	420	634	420	714	420	746					420	833	420	913
AISI 316 L	0.003	206	0.003	342	0.003	360	0.003	398	0.003	412	0.003	449				
	45	272	45	395	45	414	45	454	45	457	45	486				
T = 400° C	70	298	70	411	70	437	70	473	70	472.6	70	511				
	470	301	470	426	470	449	470	482	470	485	470	520				

TABLE 2

	$\varepsilon_1 = 0.2\%$		$\varepsilon_2 = 3.7\%$		$\varepsilon_3 = 5.5\%$		$\varepsilon_4 = 7.2\%$		$\varepsilon_5 = 9\%$		$\varepsilon_6 = 10.7\%$	
$\dot{\varepsilon}(s^{-1})$	σ(MPa) EXPER.	CALCUL.	σ(MPa) EXPER.	CALCUL.	σ(MPa) EXPER.	CALCUL.	σ(MPa) EXPER.	CALCUL.	σ(MPa) EXPER.	CALCUL.	σ(MPa) EXPER.	CALCUL.
0.004	267	318	388	398	422	438	455	477	484	518	512	555
0.082	306	333	430	413	466	453	502	493	529	533	557	572
0.88	357	350	470	432	504	472	535	511	563	552	595	590
4.5	371	366	494	449	527	490	565	529	593	570	624	608
45	368	397	493	482	530	524	567	564	605	604	631	642
480	430	445	547	534	585	576	611	616	638	657	672	693
750	471	456	574	545	605	588	635	628	659	669	683	705

TABLE 4

AISI 316 H at 20° C

COMPARISON OF CALCULATED WITH EXPERIMENTAL VALUES

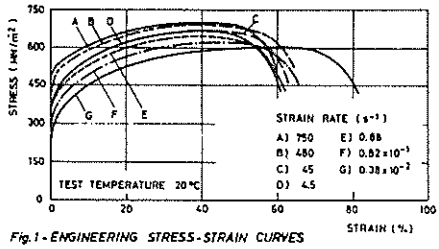

Fig. 1 - ENGINEERING STRESS-STRAIN CURVES FOR AISI 316-H AS RECEIVED STAINLESS STEEL

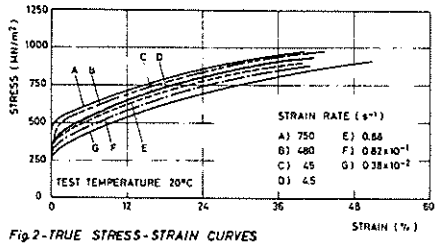

Fig. 2 - TRUE STRESS - STRAIN CURVES FOR AISI 316-H AS RECEIVED STAINLESS STEEL

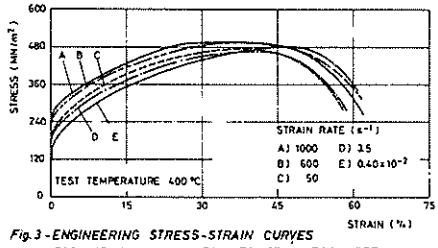

Fig. 3 - ENGINEERING STRESS-STRAIN CURVES FOR AISI 316-H AS RECEIVED STAINLESS STEEL

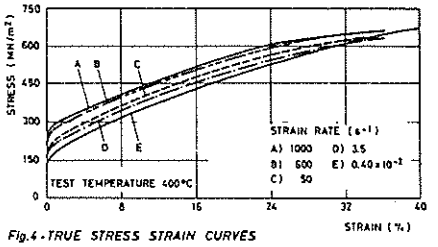

Fig. 4 - TRUE STRESS STRAIN CURVES FOR AISI 316-H AS RECEIVED STAINLESS STEEL

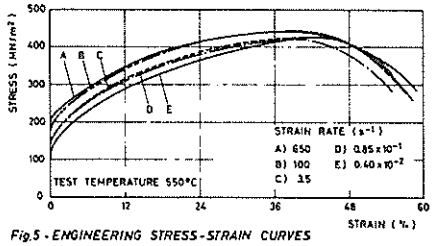

Fig. 5 - ENGINEERING STRESS-STRAIN CURVES FOR AISI 316-H AS RECEIVED STAINLESS STEEL

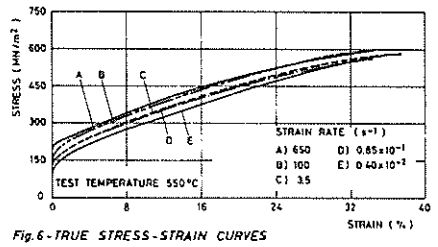

Fig. 6 - TRUE STRESS - STRAIN CURVES FOR AISI 316-H AS RECEIVED STAINLESS STEEL

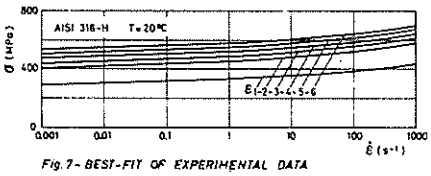

Fig. 7 - BEST-FIT OF EXPERIMENTAL DATA

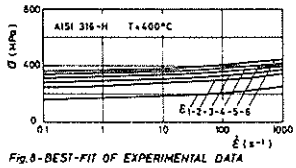

Fig. 8 - BEST-FIT OF EXPERIMENTAL DATA

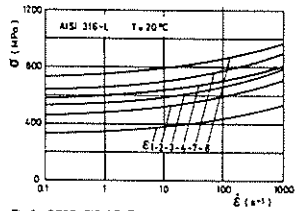

Fig 9 - BEST-FIT OF EXPERIMENTAL DATA

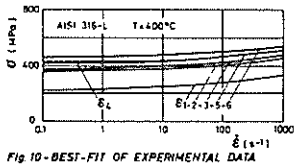

Fig. 10 - BEST-FIT OF EXPERIMENTAL DATA

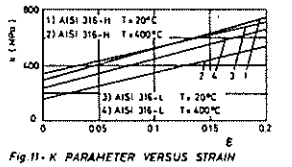

Fig. 11 - K PARAMETER VERSUS STRAIN

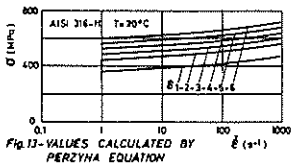

Fig. 13 - VALUES CALCULATED BY PERZYNA EQUATION

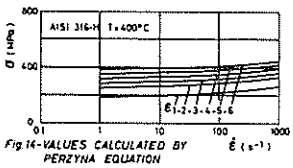

Fig. 14 - VALUES CALCULATED BY PERZYNA EQUATION

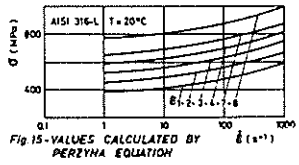

Fig. 15 - VALUES CALCULATED BY PERZYNA EQUATION

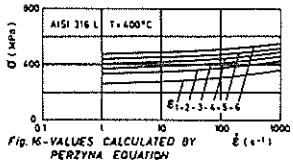

Fig. 16 - VALUES CALCULATED BY PERZYNA EQUATION

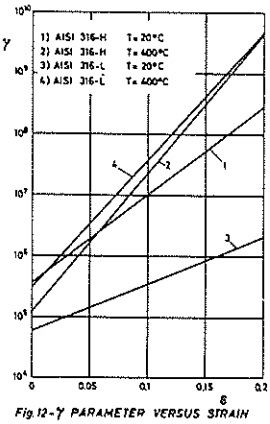

Fig. 12 - γ PARAMETER VERSUS STRAIN